

Probing Difference in Diffusivity of Chloromethanes through Water Ice in the Temperature Range of 110–150 K

Jobin Cyriac and T. Pradeep*

DST Unit on Nanoscience, Department of Chemistry and Sophisticated Analytical Instrument Facility, Indian Institute of Technology Madras, Chennai, India - 600 036

Received: December 7, 2006; In Final Form: March 30, 2007

In this work, we have examined the diffusive mixing of chloromethanes in different molecular solids H₂O, D₂O, and CH₃OH by monitoring their chemical sputtering spectra due to the impact of Ar⁺ ions in the collision energy range of 3–60 eV, focusing on amorphous solid water. The chemical sputtering spectra have been monitored over the temperature window accessible by liquid nitrogen, and the coverages of the molecules of interest and ice have been varied from one to several hundred monolayers. Instrumentation and sensitivity of the technique have been discussed. It is found that while the diffusion of CCl₄ in the molecular solids investigated is hindered, other chloromethanes such as CHCl₃ and CH₂Cl₂ undergo diffusive mixing over the same temperature range. Quantitatively, while ~4 monolayers (ML) of ice are found to block CCl₄ diffusion, the numbers are ~250 and ~600 ML for CHCl₃ and CH₂Cl₂, respectively. Crystallinity of ice does not have any effect on the diffusivity of water molecules when it is deposited below the chloromethanes. The effect of substrate was insignificant, and the rise in temperature increased diffusive mixing wherever the process was observed at a lower temperature.

Introduction

Enduring interest in the physics and chemistry of ice is due to its environmental, interstellar, and biological importance. Ice particles play an important role in the atmospheric chemistry of our planet by providing appropriate surfaces for heterogeneous catalysis. Studies on the interaction of halocarbons, especially chloromethanes with ice particles, have accelerated with the discovery of the role of ice surface in the polar stratospheric ozone depletion during spring.¹ Several techniques have been employed to study the surface structure and morphological changes of solid water. Many research groups have studied the interaction of molecules with ice particles using temperature programmed desorption mass spectrometry (TPDMS).^{2–5} Reflection absorption infrared spectroscopy (RAIRS) is especially useful to study nascent ice surface,⁶ kinetics of adsorption/decomposition,⁷ and heterogeneous catalysis.⁸ Another technique, namely, secondary ion mass spectrometry (SIMS), has emerged as one of the most surface-sensitive techniques and is being used for studying molecular solids. Temperature-programmed time-of-flight SIMS (TP-TOF-SIMS) has been used to study differences in the hydration of polar and nonpolar molecules as a function of temperature.^{9,10} An alternative to SIMS is low-energy surface scattering or so-called chemical sputtering (CS).¹¹ This is also called as low-energy sputtering (LES), which has also been used for surface studies.¹² This is a hyper-thermal energy process in which charge exchange occurs upon the collision of ions in the energy range of 10–100 eV and surface species are released as ions or neutrals. The ionization potential of the projectile ion is an important parameter in determining the secondary ion yield and the method has been used extensively in understanding molecular surfaces such as self-assembled monolayers.¹³ Associated

reactive collisions have been extremely informative in surface characterization.^{14–17} Low-energy projectile ions are very good probes for monitoring surface properties of ice or other molecular solids by themselves undergoing reactive collisions. By looking at the resultant mass spectra, it is possible to characterize the surface of interest. The reactions happen at ice surfaces are unique and significantly different from their liquid state analogues.¹⁸

The efficiency of chemical sputtering depends on the physical and chemical properties of the projectiles and the surface involved in the process. This technique can be made use of for examining the diffusion of molecules through molecular solids. Chemical sputtering of species present on the surface will give a clear understanding of the processes like diffusion, migration, and proton transfer happening at the first few monolayers of the surface. In this paper, we discuss the sputtering of surface molecules, due to the collision of low-energy Ar⁺ ions at different molecular solids. Chemical sputtering or low-energy sputtering has many advantages over other techniques such as TPD and SIMS, which are widely used in the surface studies of molecular solids. In TPD, the information obtained is only about the desorbing molecule, and one does not know precisely about the fate of molecules before desorption, especially when some molecule is buried over the other. SIMS is a destructive technique, because a high-energy projectile can penetrate several tens of monolayer (ML) of the surface. Therefore, it is difficult to get the surface information of thin molecular films. As a result, chemical sputtering is one of the important techniques to study the microscopic processes on ice surfaces. Argon, hydrogen, and helium ions are good projectiles for low-energy sputtering.^{19–21} Molecular beam experiments and molecular dynamic simulation have been conducted to explore the dynamics of argon atom collisions with water ice.²² For thermal incident energies, the scattering is almost entirely due to trapping followed by thermal desorption, and direct inelastic scattering

* Corresponding author. E-mail: pradeep@iitm.ac.in. Fax: +91-44-2257 0509/0545.

is observed at higher energies. The results suggest that low-energy collisions of argon leads to effective transfer of energy to the surface.

Chloromethane/ice system has been chosen in the present study due to its atmospheric/environmental relevance. The composition and morphology of stratospheric ice particles are related to their history of formation. In the present context, the chemistry of chloromethanes on ice particles is controlled by their molecular and transport properties at the surface. Both theoretical and experimental studies have on the halomethane/water ice system.²³ From a fundamental point of view, ice surface is a model system for molecular solids since extensive experimental and theoretical data on intermolecular interactions are available.^{24,25} Ice can exist in a number of structurally different forms, depending on the pressure and temperature. Mainly two different forms of ice, crystalline (CW) and amorphous solid water (ASW) can be formed on a cold substrate in vacuum by vapor deposition at different temperatures. Slow condensation of vapor below 130 K results in low density amorphous ice (density < 0.93 g/cm³).²⁶ Structure and morphology of amorphous H₂O and D₂O have been extensively studied by different techniques. The TPD of CCl₄ from ASW film shows two distinct desorption states, near 130 and 145 K.²⁷ It is found that overlayers of ASW delay the desorption of CCl₄ until the onset of crystallization.³ Combined study of TPD and RAIRS reveals that up to its desorption temperature of 140 K, CHCl₃ remains immobile in the crystalline ice surface.²⁸ But CHBr₃ shows surface diffusion in the temperatures as low as 85 K. Aoki et al. show that the CHCl₃ molecules are adsorbed on the topmost ice layer mainly through weak electrostatic interactions with their H atoms oriented toward the substrate at 35 K.²⁹ Further, upon heating of the substrate just below the desorption temperature (120 K), the molecules are found to migrate from the topmost layer to the inner layers owing to thermal diffusion. There is no report available on the solid state interaction of CH₂Cl₂ with ice.

We have been interested in the surface chemistry of ice under well-defined conditions and this work is partly motivated by the earlier studies.^{30,31} The desire to get more insight into the diffusion properties of CCl₄ and other chloromethanes lead to the present study. A deeper understanding of the diffusion of such molecules is vital in several areas of science including fundamental research.

Experimental

Figure 1 shows an overview of the ion-scattering instrument fabricated for the present study. The entire vacuum system is composed of two main chambers and a sample manipulator. The interior surface of the chamber was polished to reduce out-gassing. Each region of the system is pumped by a Pfeiffer (TMU 261) 210 L/s turbomolecular drag pump. These two turbo pumps are backed by another Pfeiffer 60 L/s pump (TMU 071P) and further by a Pfeiffer dry pump (MVP 055). This ensures a hydrocarbon-free environment, although some fluorocarbon fragments were detected probably due to the lubricant used in the turbomolecular pump. The pressure in each chamber is measured using Bayard-Alpert type (PBR 260) ionization gauges controlled by a "Multi-gauge" vacuum gauge controller (Pfeiffer, Model TPG 256 A). An ultimate pressure below 0.5×10^{-10} mbar (limit of the controller) was achieved in both the ionization and scattering chambers after bake-out. During the experiment, the sample vapors, i.e., water, CCl₄, etc., were introduced into the scattering chamber via a variable leak valve (VG England). The sample line was pumped by a rotary pump, and the samples

were separated from the sample line by open-close valves (Swagelok). The ionization chamber and surface-scattering chamber are separated by a differential pumping baffle, and the ions are transferred from the ionization region to the scattering region via the quadrupole mass filter (Q1). The alignment of ion optical components was achieved using standard laser transit procedures. Argon gas was introduced into the ionization chamber through another leak valve during which the pressure in it was raised to 1.0×10^{-7} mbar. The pressure measured in the scattering chamber during experimental condition, i.e., when the Ar source was opened was $\sim 4.0 \times 10^{-9}$ mbar, which was an indication of effective differential pumping.

A high precision UHV specimen translator (Thermo Electron Corporation) with xyz axis movement and tilt facility is used as the surface holder. The substrate holder is made of OFHC copper, and the rest of the spectrometer is made with nonmagnetic stainless steel. The mounting plate can be removed without disturbing the drive and is electrically isolated from the supporting structure. The heating element (H) is a molybdenum sheet. A 10×10 mm polycrystalline copper sheet is used as the substrate for deposition in this experiment. The heater is electrically isolated from the rest of holder by sapphire balls. Two K-type thermocouples simultaneously measured the temperature. One thermocouple is kept on the molybdenum plate and other one is attached directly to the copper substrate. The copper substrate is fixed on the molybdenum plate by a thin sheet of mica. The temperature difference between these two thermocouples is less than 1 K, and the temperature gradient across the sample plate is close to zero. Sample cooling was achieved by liquid nitrogen circulation and the minimum temperature attained was 100 K. The sample plate is connected to the LN₂ sink through a flexible copper braid and the sink is connected to LN₂ supply by copper tubes. A continuous flow of LN₂ is achieved by pressurizing LN₂ with high pure N₂ gas. A temperature of 100 K can be reached within 20 min time, and the heating rate (typically 5 K/min) is controlled by a Watlow temperature controller (Model A18) and a home-built power supply.

An electron impact ionization (EI) source from ABB Extrel was used to generate positive or negative ions. These ions are extracted from the source and transferred into a quadrupole mass filter (Q1) through a set of einzel lenses. It is possible to get the projectile ions with varying collision energy from 1–100 eV by varying the potential of the ion source block and tuning the rest of the ion optics to get a beam current of 1–2 nA. The desired mass-to-charge ratio is allowed to pass through Q1. The ions collide with the surface at an angle of 45° with reference to the surface normal. The secondary ions generated by the ion collision are then collected by a quadrupole mass analyzer (Q3). All the quadrupoles and control electronics are from Extrel Core Mass Spectrometry. The analyzer quadrupole is kept at a nominal scattering angle of 90° with reference to the incident ion beam direction. All the experiments reported here were conducted by selecting Ar⁺ (*m/z* 40) by Q1.

Every experiment begins with the cleaning of the substrate. Volatile impurities are removed by heating of substrate to a temperature of 400 K for 10 min. Then the substrate was rapidly cooled to 110 K and kept at that temperature for 10 min. Before depositing the sample molecule, the substrate was again heated to 220 K for 10–20 s to avoid any kind of condensation on the substrate plate during the cooling process. After this procedure, substrate has cooled back to the required temperature for the experiments. Thus, the experimental procedures ensured the removal of any kind of impurity condensing on the substrate.

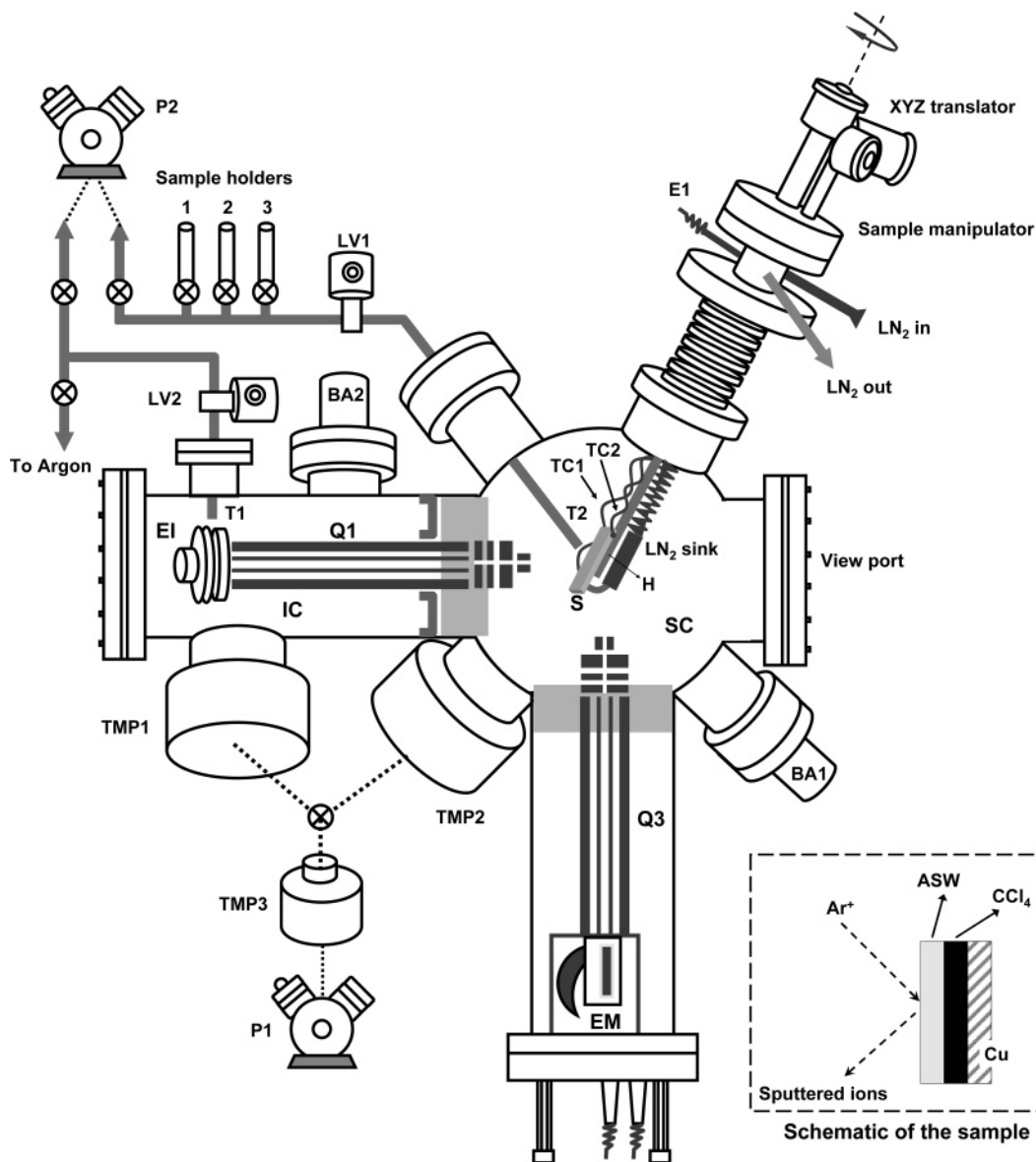


Figure 1. Schematic of the vacuum chamber and ion-scattering setup. TMP1, TMP2, and TMP3 are two 210 and one 60 L/s turbomolecular pumps, respectively. P1 and P2 represent diaphragm pumps. Q1 is the mass filter quadrupole and Q3 is the analyzer quadrupole. LV1 and LV2 are the leak valves on the sample line. BA1 and BA2 are BA type vacuum gauges for measuring the vacuum in the scattering chamber (SC) and ionization chamber (IC), respectively. T1 is the probe for admitting Ar gas directly into electron impact ionizer (EI), and T2 is used for introducing sample vapors. S is the polycrystalline copper substrate. EM represents the electron multiplier assembly of the system, and E1 is the electrical feed-through for thermocouple (TC1 and TC2) and resistive heater (H). The manipulator is perpendicular to Q1 and Q3, but shifted in the schematic for clarity.

However, there can be contamination due to the background gas as a typical experiment lasted for 15–20 min, and during which a deposition of <0.1 ML (assuming a partial pressure of 10^{-10} mbar for condensable gases) is expected. Test experiments were conducted to check the efficiency of the instrument in detecting surface species and a summary of the data is given in Supporting Information S1. These results support the surface sensitivity of the technique.

All liquids, H_2O , D_2O , CCl_4 , CHCl_3 , CH_2Cl_2 , $\text{C}_2\text{H}_2\text{Cl}_4$, and CH_3OH , were purified by several freeze–pump–thaw cycles on each day of the experiment before use. These chemicals were purchased from Aldrich chemicals and deionized water was used after triple distillation for preparing solid water. Surfaces for the studies were prepared by the deposition of the corresponding vapors, which were introduced onto the sample plate through a leak valve. The gas-line was pumped thoroughly to avoid contamination. The distance between the sample source tube

and copper substrate was adjusted in order to obtain uniform sample growth on the substrate. The deposition flux of the vapors was adjusted to ~ 0.1 ML/s. The thickness of the overlayer was estimated assuming that 1.33×10^{-6} mbar/s = 1 ML. In all the experiments, the deposition temperature was kept at 110 K. The partial pressure(s) of the gas(es) inside the scattering chamber during deposition time was 1×10^{-7} mbar. After deposition of a given molecule A, a 5 min delay was allowed before the deposition of the next molecule B, to prepare A@B (the symbolism implies the creation of a layer of B over A). This was to ensure that B was free from any contamination by A. We prepared several systems for studying diffusive miscibility of chloromethanes. For example, 50 ML of CCl_4 was deposited first on Cu substrate followed by 50 ML of ASW, resulting in CCl_4 @ASW, which was used for the study of CCl_4 diffusion through ice overlayers. The other systems for study were also prepared in the same manner. The ice film grown

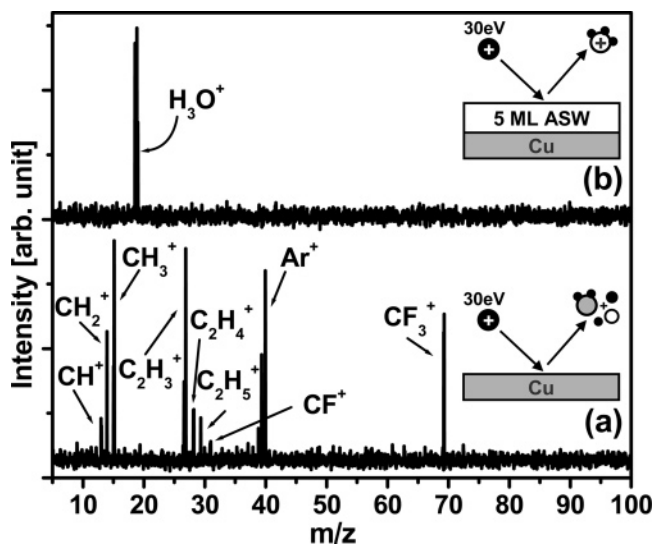


Figure 2. (a) Chemical sputtering spectra from the Cu surface at 110 K and (b) after 5 ML coverage of ASW on Cu at 110 K. Total disappearance of hydrocarbon features in panel b shows the surface sensitivity of the technique. Collision energy of Ar^+ ion was 30 eV in both the cases. CF_3^+ and CF^+ features indicate the presence of fluorocarbons as a result of residual contamination. Low-energy chemical sputtering is highly sensitive to fluorocarbons. A schematic of the collision event is shown with each spectrum.

this way in ultrahigh vacuum is known to be amorphous in nature (ASW) while the deposition above 140 K results in crystalline ice (CW).^{32,33} Polycrystalline copper was used earlier as the substrate material for preparing amorphous and crystalline ice films.³⁴ The other molecular solids discussed in this paper do not have any phase or structural transformation in the temperature range of 100–200 K.

After making the system, the surface was subjected to collision with Ar^+ ions and the resultant sputtering species gave information about the molecules at the surface. The temperature dependence of molecular diffusion was investigated by rising the temperature at 5 K/min and monitoring of sputtering spectrum as a function of temperature. Ar^+ ions of 3–60 eV collision energy were used as projectile ions in all the experiments. Surface contamination due to Ar^+ ion was nil during the experiments since argon does not deposit on the surface at this temperature. This is one advantage over the other projectiles like Cs^+ that are frequently used in low-energy chemical sputtering.^{2,35} After the experiments, a simple bake-out of the chamber will give a clean surface for the next experiment. All the spectra presented here are averaged for 50 scans, and the peak intensities were normalized to that of 3 eV Ar^+ ion scattering from Cu at 110 K.

The surface sensitivity of the technique can be demonstrated by investigating the chemical sputtering spectra of Cu surface at 110 K and 5 ML ASW deposited on Cu at the same temperature. The sputtered ions due to hydrocarbons on the copper surface are visible at 110 K (Figure 2a). A small amount (<0.5 ML) of hydrocarbon is expected on the copper surface as we have not done a high temperature cleaning processes. But 5 ML coverage of ASW on the copper surface makes all hydrocarbon features to disappear completely. The detection of very small amount of hydrocarbons as well as the disappearance these peaks due to an overlayer of 5 ML water demonstrates the sensitivity of the technique. Note that the hydrocarbon intensities vary depending on the history of the sample as expected. Isotope intensities are not truly represented in the data presented.

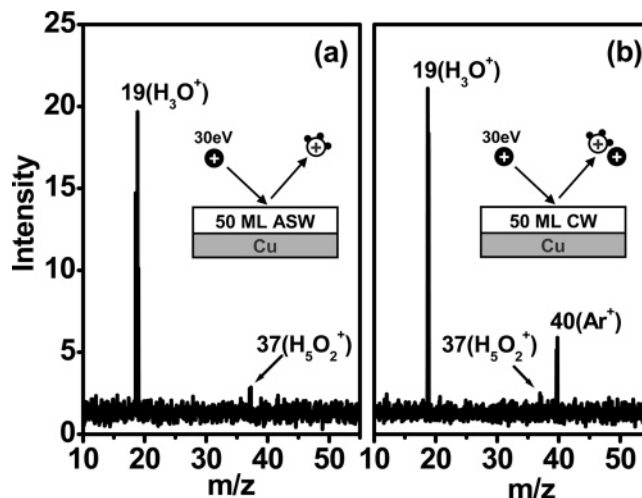


Figure 3. Comparison of the intensity of sputtered H_3O^+ (m/z 19) peak from (a) ASW at 110 K and (b) CW at 145 K. CW has prepared by annealing ASW at 155 K and then cooling back to 145 K to measure the chemical sputtering spectra.

Results and Discussion

Figure 3 shows the chemical sputtering spectra for amorphous solid water (ASW) and crystalline water (CW) at 30 eV collision energy. At lower collision energies of 3–20 eV, the projectile ion Ar^+ is scattered from these surfaces without any secondary ion yield. But the intensity of Ar^+ ion peak ($40 m/z$) reduces as the energy of the projectile ion increases. This reduction in intensity is mainly due to trapping and neutralization of Ar^+ ions at the surface. The chemical sputtering from the molecular surface starts at 25 eV onward and is observable in the resultant mass spectra. In the case of ASW or CW surfaces, the emergence of sputtering peak, i.e., H_3O^+ (m/z 19) begins above 25 eV collisions. It is important to note that protonated molecular ions of water are created as a consequence of proton-transfer reaction [$2\text{H}_2\text{O} \rightarrow \text{H}_3\text{O}^+ + \text{OH}^-$] upon the collision of Ar^+ ions.³⁶ The H_3O^+ ($19 m/z$) peak alone is observed in the spectra and H_2O^+ peak is totally absent throughout the energy range of 20–60 eV. The structural differences in these ice surfaces are also visible in the sputtering features. Figure 3a shows a peak at m/z 19, while Figure 3b contains a feature at m/z 40 along with the peak at m/z 19. The absence of the peak at m/z 40 for ASW surface can be explained as its efficient trapping in comparison to CW.^{22,37} The peak at m/z 37 is due to $(\text{H}_2\text{O})\text{-H}_3\text{O}^+$.

The diffusivity of CCl_4 through ice was investigated by preparing 50 ML CCl_4 @50ML ASW system. The chemical sputtering spectra of this system is presented in Figure 4, which shows the absence of CCl_4 features in the whole range of collision energies. In comparison, chemical sputtering of bare CCl_4 surface gives CCl_3^+ , CCl_2^+ , CCl^+ , and Cl^+ , which appear above 25 eV collision energy (Supporting Information S2). In order to check the temperature effect on 50 ML CCl_4 @50ML ASW system, the temperature was increased at a heating step of 5 K/minute with simultaneous monitoring of the sputtered species at 30 eV collision energy. The collected spectra contain the H_3O^+ features alone along with $\text{H}_2\text{O}(\text{H}_3\text{O})^+$ till 150 K. Water desorption from the surface is significant above 150 K and this prevents the measurement of quality data.³⁸ Therefore, it is difficult to get the diffusion behavior of molecules through water ice above this temperature. This limitation prevented us from detecting the CCl_4 desorption at 165 K, discussed in Smith et al.³ The desorption of CCl_4 molecules at ~ 160 K was visible in the rise in the vacuum level but it could not be detected in

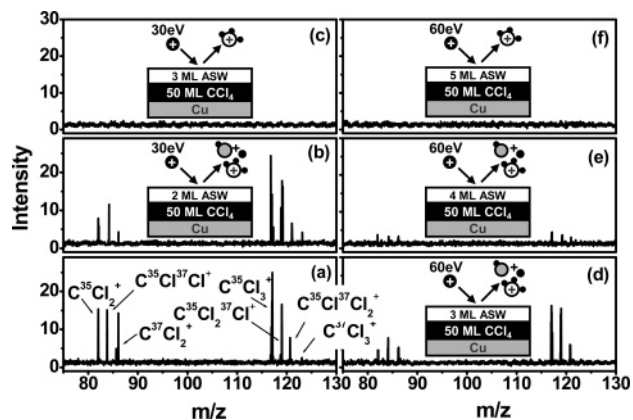


Figure 7. Effect of H₂O thickness on the diffusive mixing of 50 ML CCl₄ deposited on copper substrate. (a) CCl₄@1 ML ASW, (b) CCl₄@2 ML ASW, and (c) CCl₄@3 ML ASW at 30 eV collision of Ar⁺ ion. Panels d, e, and f represent 60 eV collision of Ar⁺ ions at CCl₄@3 ML ASW, CCl₄@4 ML ASW and CCl₄@5 ML ASW, respectively. At 30 eV collision, CCl₄ features are not observed for 3 ML coverage of ASW due to poor penetrating power of the projectile, whereas at 60 eV it disappeared at 5 ML coverage. Spectrum in the relevant region is only shown and the temperature was 110 K for all spectra.

is clear that 3 ML coverage of ASW is enough to eliminate CCl₄ features when probed with Ar⁺ ion of 30 eV energy. As expected, the increase of projectile energy to 60 eV gives the characteristic CCl₄ peaks, due to greater ion penetration. We can conclude that 3–4 ML of ASW block the diffusion of CCl₄ molecule.

The next question we seek to address is whether the phenomenon observed could be a result of the immiscible nature of the CCl₄/water system. For studying this, we have done the same experiment with 50 ML ASW@50 ML CCl₄ system. The spectra, in this case, contain peaks at *m/z* 19, which is due to H₃O⁺ along with CCl₄ features (Supporting Information S3). So the water molecules can penetrate through CCl₄ overlayers or the voids created in the CCl₄ matrix are available for H₂O diffusion whereas CCl₄ diffusion is not possible through ASW. These observations lead us to the conclusion that CCl₄ molecules cannot diffuse through the hydrogen-bonded network of ASW. This argument agrees well with the non-fragile nature of ASW below 150 K, reported by McClure et al.³⁹ The TPD experiments conducted in this reference shows that the intermixing occurs near 150–160 K as a result of crystallization. The glass transition temperature of amorphous water is still in debate,^{39,40} and our observation supports the suggestion, although indirectly, that water undergoes transition only above 150 K. The absence of CCl₄ features in the temperature range 110–150 K suggests that ice overlayer is not undergoing a structural rearrangement that leading to crystallization. The experiment on CCl₄@CH₃-OH shows that CCl₄ is not undergoing diffusion through CH₃-OH overlayers also. CH₃OH is also known to form hydrogen-bonded network in the solid state, which prevents CCl₄ diffusion.⁴¹ The microporous ice may contain a number of connected pathways.⁴² The number of connected pathways in ASW film decreases rapidly if the thickness is larger than 60 ML. It is believed that the low-temperature desorption of CCl₄ arises through these pathways.³ But the present experimental results show that CCl₄ cannot penetrate through the hydrogen-bonded network of the ice films thicker than 4 ML. Again, ASW presents a barrier for C₂H₂Cl₄ also, as a similar situation is encountered in 50 ML C₂H₂Cl₄@50 ML ASW. As in the case of CCl₄, the C₂H₂Cl₄ features are not seen above

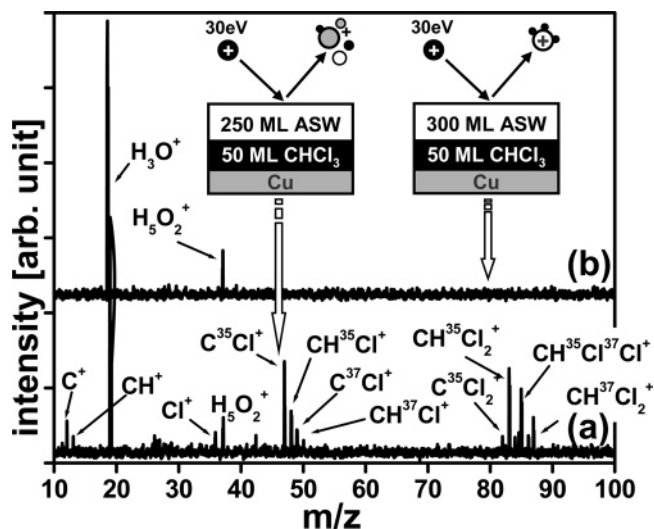


Figure 8. Spectra showing the difference in diffusive mixing of CHCl₃ molecule at two different coverages of ASW. (a) 250 and (b) 300 ML. At 300 ML, CHCl₃ diffusive mixing is stopped, and spectrum b contains only H₃O⁺ and (H₂O)H₃O⁺ peaks whereas at 250 ML, all the peaks due to CHCl₃ are present.

4 ML coverage of ASW. It appears that transverse diffusion of tetrachloroethane molecule through ice is hindered due to its bigger size.

Experiments with CHCl₃ and CH₂Cl₂ have been conducted in the same way to investigate the transport properties of these chloromethanes in ASW overlayers. For this purpose, we have prepared the systems, CHCl₃@ASW and CH₂Cl₂@ASW, and the thicknesses of the molecular solids were kept constant at 50 ML. Interestingly, diffusive mixing was observed in both the cases. This mixing can be terminated at some point by increasing the rate of deposition and by increasing the thickness of the solute layer to large values. In order to study the effect of thickness on this process chemical sputtering spectra were collected from the surface after increasing the thickness of the upper layer by 10 ML in a systematic manner. Experiments revealed that signatures of CHCl₃ and CH₂Cl₂ on the top layers disappeared at 300 and 650 ML, respectively. It is difficult to infer the exact coverage at which these underlying molecules are prevented from reaching the upper layers. But it is certain that the presence of CHCl₃ was detectable at 250 ML ASW coverage and at 300 ML it was completely absent. This is shown in Figure 8. The 300 ML spectrum does not contain any CHCl₃ sputtering peaks (Figure 8b) whereas 250 ML coverage showed peaks due to CHCl₃ (Figure 8a). For CH₂Cl₂, the intensities of the solutes disappear between 600 and 650 ML and the coverage dependence of chemical sputtering spectra is shown in Figure 9. Peaks at *m/z* 47, 49, and 51 along with 48 and 50 confirm the presence of CH₂Cl₂ at the surface. Thus, we can summarize that mixing of CH₂Cl₂ and CHCl₃ is incomplete with increase in the thickness of H₂O layers. The mixing is primarily due to the transverse diffusion of H₂O molecules during the time of deposition of chloromethanes, CH₂Cl₂ and CHCl₃. The diffusive mixing of CHCl₃ with other molecular solids D₂O, CCl₄, and CH₃OH, was also checked (Supporting Information S4). The chemical sputtering spectra showed that CHCl₃ undergoes diffusive mixing with these molecular solids also. The miscibility is more in CHCl₃@CCl₄ system as it is evident from the peak intensities.

The next step was to study the nature of the substrate on the phenomenon reported. In order to check the substrate effect, we have covered the copper substrate with another molecular

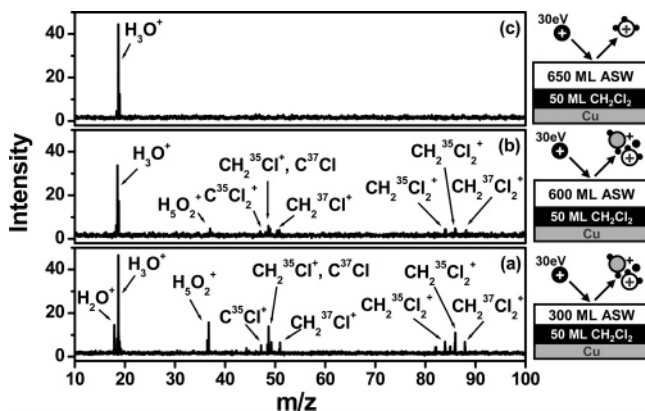


Figure 9. Diffusive mixing of 50 ML CH_2Cl_2 at varying coverages of H_2O . Panels a, b, and c are the chemical sputtering spectra at different coverages 300, 600, and 650 ML of ASW, respectively. Collision energy of Ar^+ ion was 30 eV, and the temperature was 110 K. Complete disappearance of the CH_2Cl_2 peaks occur at 650 ML of ASW.

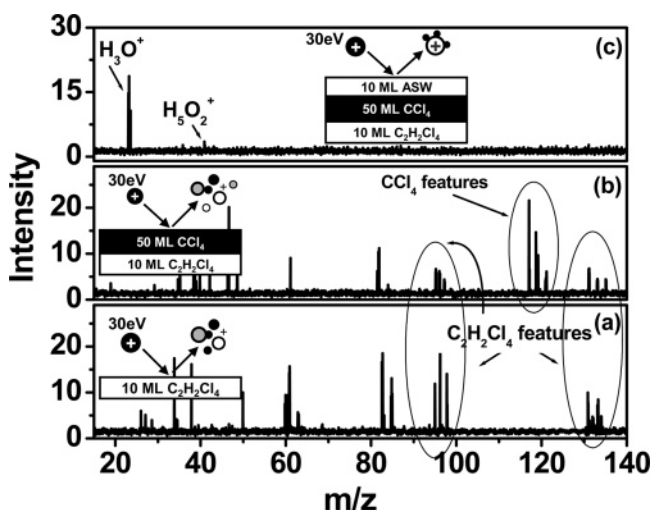


Figure 10. The effect of substrate on the chemical sputtering spectra. (a) 10 ML $\text{C}_2\text{H}_2\text{Cl}_4$ alone, (b) 10 ML $\text{C}_2\text{H}_2\text{Cl}_4$ @50 ML CCl_4 and (c) 10 ML $\text{C}_2\text{H}_2\text{Cl}_4$ @50 ML CCl_4 @10 ML ASW. (b) Sputtering peaks due to both CCl_4 and $\text{C}_2\text{H}_2\text{Cl}_4$; (c) all these characteristic peaks are absent, and only H_3O^+ and $\text{H}_2\text{O}(\text{H}_3\text{O})^+$ are present. The temperature is 110 K for all spectra. Copper surface has been omitted in the schematic for clarity.

solid having a higher desorption temperature. The molecule selected was 1,1,1,2-tetrachloroethane ($\text{C}_2\text{H}_2\text{Cl}_4$) because the desorption temperature of $\text{C}_2\text{H}_2\text{Cl}_4$ is 185 K, higher than water desorption temperature in the present experimental conditions. Before preparing the CCl_4 @ASW system, the sample substrate was covered by depositing 10 ML $\text{C}_2\text{H}_2\text{Cl}_4$ molecules, followed by deposition of CCl_4 and ASW, to make CCl_4 @ASW. Chemical sputtering data from this surface is shown in Figure 10. There were no CCl_4 sputtering features from $\text{C}_2\text{H}_2\text{Cl}_4$ @ CCl_4 @ASW system in the entire temperature range of 110–150 K. But mixing of $\text{C}_2\text{H}_2\text{Cl}_4$ and CCl_4 was clearly observable in the spectra after deposition of CCl_4 over $\text{C}_2\text{H}_2\text{Cl}_4$ (in $\text{C}_2\text{H}_2\text{Cl}_4$ @ CCl_4). Figure 10a shows the chemical sputtering spectrum from 10 ML $\text{C}_2\text{H}_2\text{Cl}_4$ and the peaks observed, namely, $\text{C}_2\text{H}_2\text{Cl}_3^+$ and $\text{C}_2\text{H}_2\text{Cl}_4^+$, are the characteristic features of $\text{C}_2\text{H}_2\text{Cl}_4$. We take m/z 131 and 166 as the characteristic features even though m/z 83 and 85 m/z are the 100% peaks of $\text{C}_2\text{H}_2\text{Cl}_4$, as this region does not interfere with the CCl_4 features. The peaks due to $\text{C}_2\text{H}_2\text{Cl}_3^+$ and $\text{C}_2\text{H}_2\text{Cl}_4^+$ are present along with those of CCl_3^+ in Figure 10b due to the mixing of two layers, $\text{C}_2\text{H}_2\text{Cl}_4$ and CCl_4 , as discussed earlier. After this

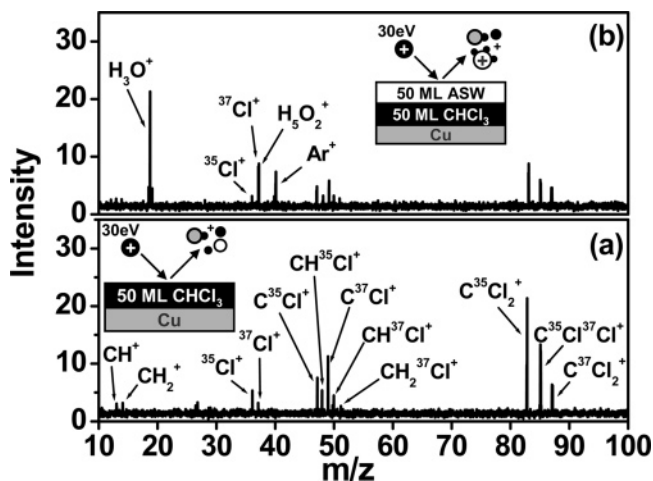


Figure 11. Sputtering spectra of 50 ML CHCl_3 and 50 ML CHCl_3 @50 ML ASW at 30 eV collision of Ar^+ ion. There is a reduction in the intensity of CHCl_3 peaks upon H_2O deposition, which is a direct measure of the composition at the surface.

analysis, ASW was deposited on the same surface and then analyzed by the usual manner. The spectra do not contain either CCl_3^+ or $\text{C}_2\text{H}_2\text{Cl}_3^+$ peaks. Also, the chemical sputtering spectra of ASW@ CCl_4 @ASW system do not contain any CCl_4 features. These control experiments confirm that the copper substrate does not play a role in the sample preparation process. Further, we examined the effect of deposition rate by conducting deposition of water vapor at three different pressures, 5.0×10^{-8} , 1.0×10^{-7} and 5.0×10^{-7} mbar to prepare 50 ML CHCl_3 @50 ML ASW. The intensities of the sputtered peaks were comparable in all these cases (Supporting Information S5). Hence, the rate of deposition does not affect the data significantly in the range investigated.

From these experiments, it is clear that CCl_4 gets trapped beneath the ASW layers, and other chloromethanes, namely, CHCl_3 and CH_2Cl_2 , are undergoing diffusive mixing. It is shown that ASW is not a barrier material for CH_2Cl_2 and CHCl_3 . The observation presented here is in contrast to the results of McClure et al.⁵ They argue that diffusion behavior of CHCl_3 is similar to CCl_4 and suggest that both CHCl_3 and CCl_4 will not be transported through ice in the range of 110–130 K. To check various possibilities, we have conducted experiments with CH_3OH @ CCl_4 and CH_3OH @ASW. As expected, CH_3OH readily diffuses through amorphous ice films. The sputtering peak at 33 m/z (CH_3OH_2^+) shows the diffusive mixing of CH_3OH in these films. Another experiment with 50 ML CH_3OH @50 ML CCl_4 @50 ML ASW showed that the CCl_4 layer is not hindering the transport of CH_3OH to top layers of ASW. Thus, CCl_4 layer has adequate pores for molecular transport. The chemical sputtering from 50 ML CH_3OH @50 ML CCl_4 @50 ML ASW and 50 ML ASW @50 ML CCl_4 @50 ML CH_3OH contains the peaks due to both CH_3OH_2^+ and H_3O^+ . Thus molecular transport through CCl_4 is possible in either direction.

The composition of the mixed layers can be roughly estimated by comparing the peak intensities of the species before and after mixing. Figure 11 shows the chemical sputtering spectra of CHCl_3 surface before and after depositing 50 ML of ASW overlayers. The intensity ratio of the peaks of CHCl_2^+ from two surfaces (50 ML CHCl_3 and 50 ML CHCl_3 @50 ML ASW) is less than 4. This observation leads us to the conclusion that at the surface layer, volume ratio of CHCl_3 is $\leq 25\%$.

The effect of change in temperature could not be differentiated at lower coverages (<10 ML). But the increase in temperature affects the diffusive mixing at higher coverages. For example,

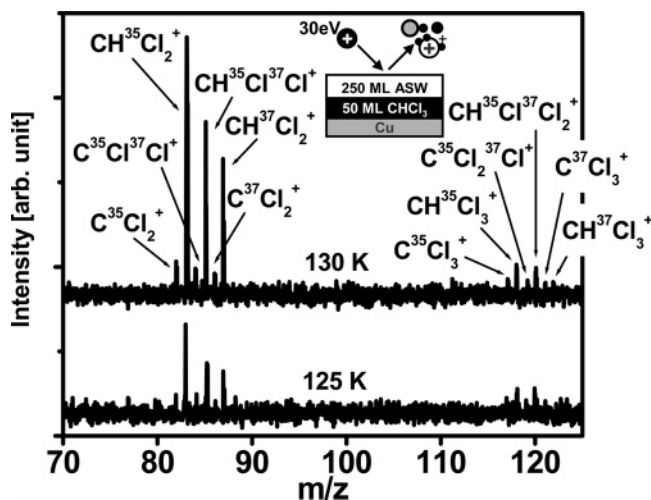


Figure 12. The intensities of the CHCl_2^+ and CHCl_3^+ peaks are increased due to the change in concentration of CHCl_3 on the surface with raise in temperature. The projectile ion is 30 eV Ar^+ , and the system is 50 ML CHCl_3 @250 ML ASW. With the temperature rise from 125 K (lower trace) to 130 K (upper trace), more CHCl_3 is diffusing through ice overlayers. The tiny peaks in the left side of CHCl_2^+ and CHCl_3^+ are due to CCl_2^+ and CCl_3^+ ions formed from CHCl_3 .

the intensity of the peaks due to the underlying molecule increases with increase in temperature. The diffusion of CHCl_3 was little for 250 ML of ASW at 110 K but an increase in the temperature does provide more energy for transverse diffusion for the CHCl_3 molecules. Thus the buried CHCl_3 molecules can be transported through the ASW layers and their presence is visible in the chemical sputtering spectra (Figure 12). A temperature-dependent study of 50 ML CHCl_3 @250 ML ASW shows a small decrease in the intensity of CHCl_2^+ peaks at 120 K, compared to that obtained at 110 K. But a temperature rise from 120 to 130 K gives a fairly large increase in the intensity of the same peaks. Initial decrease may be due to the lateral diffusion of CHCl_3 . Heating the sample above 120 K results in the reorganization of the “topmost surface” layers of ASW film leading to the collapse of micropores.³³ Thus more CHCl_3 molecules are coming out from the pores. It appears that while temperature-dependent reorganization at 120 K is feasible for CHCl_3 molecules, the molecular size prevents this in the case of CCl_4 . Further increase in the temperature resulted in the desorption of CHCl_3 at 135 K, and this is visible in the chemical sputtering spectrum which contains only H_3O^+ peak at m/z 19.

Summary and Conclusions

An in-house developed LES/chemical sputtering instrument has been used for studying molecular solids. The ion-scattering experiment described here demonstrates the study of diffusive mixing of three chloromethanes with water-ice. The experiments are done with ASW and the projectile ion was Ar^+ . It is shown that CCl_4 cannot diffuse through more than four overlayers of ASW. The critical size of the CCl_4 molecule appears to prevent its diffusion through ASW. But H_2O molecule can penetrate through solid CCl_4 when it is buried under solid CCl_4 . It appears that the transport of H_2O through solid CCl_4 is through cracks. The hydrogen bond network of the ASW film, however, restricts the transport of CCl_4 molecules. Other molecular solids, D_2O and CH_3OH are also acting as barriers for the diffusive mixing of CCl_4 . The smaller chloromethanes, namely, dichloromethane and chloroform, can pass through ice

and the solid state mixing occurs down to 100 K. It is clear that dynamic nature of ice and ice pores are playing important roles in the diffusivity of chloromethanes. While CCl_4 does not diffuse in ice, CHCl_3 does so. The interaction between chloromethanes and water occurs through the oxygen atom and the interaction energy is in the order, $\text{CCl}_4 > \text{CHCl}_3 > \text{CH}_2\text{Cl}_2 > \text{CH}_3\text{Cl}$. But in the solid state, the interaction energy is in the reverse order.⁴³ This is due to the change in dominant interaction from liquid state to solid state. The overall interaction between halomethanes and water is based on the combination of atomic charge of chlorine and molecular polarizability. Considering these, replacement of a Cl atom to H atom can have a significant effect in their diffusivity in ice. The diffusive miscibility of CH_2Cl_2 with H_2O stops after 600 ML coverage and for CHCl_3 , the limit is 250 ML. The absence of CCl_4 on ASW surface above 4 ML coverage is due to the hydrogen-bonded network of the non-fragile ASW film in the temperature range of 110–150 K. The results suggest that simple hydrochloromethanes could be present throughout ice particles while the presence of CCl_4 on the ice surface depends on the history of its formation. In cases where ice is deposited over CCl_4 nuclei, it is unlikely to be present on the surface, but CCl_4 deposition on ice particles will retain it there. This suggests that the results may have implications to the atmospheric chemistry of ice particles.

Acknowledgment. T.P. thanks the Department of Science and Technology for a Swarnajayanti Fellowship. J.C. acknowledges a research fellowship from the Council of Scientific and Industrial Research.

Supporting Information Available: Ar^+ ion chemical sputtering at various conditions. Spectra of (1) different surfaces, (2) 50 ML CCl_4 at different collision energies, (3) diffusive mixing of H_2O through CCl_4 overlayers, (4) diffusive mixing of CHCl_3 with other molecular solids, and (5) surfaces prepared at different deposition pressures. This information is available free of charge via the Internet at <http://pubs.acs.org>.

References and Notes

- (1) Molina, M. J.; Tso, T.-L.; Molina, L. T.; Wang, F. C. Y. *Science* **1987**, *238*, 1253.
- (2) Park, S. C.; Kang, H. *J. Phys. Chem. B* **2005**, *109*, 5124.
- (3) Smith, R. C.; Huang, C.; Wong, E. K. L.; Kay, B. D. *Phys. Rev. Lett.* **1997**, *79*, 909.
- (4) Sadtchenko, V.; Knutsen, K.; Giese, C. F.; Gentry, W. R. *J. Phys. Chem. B* **2000**, *104*, 2511.
- (5) McClure, S. M.; Barlow, E. T.; Akin, M. C.; Safarik, D. J.; Truskett, T. M.; Mullins, C. B. *J. Phys. Chem. B* **2006**, *110*, 17987.
- (6) Mate, B.; Medialdea, A.; Moreno, M. A.; Escribano, R.; Herrero, V. J. *J. Phys. Chem. B* **2003**, *107*, 11098.
- (7) Faradzhev, N. S.; Perry, C. C.; Kusmierck, D. O.; Fairbrother, D. H.; Madey, T. E. *J. Chem. Phys.* **2004**, *121*, 8547.
- (8) Gane, M. P.; Williams, N. A.; Sodeau, J. R. *J. Phys. Chem. A* **2001**, *105*, 4002.
- (9) Kondo, M.; Kawanowa, H.; Gotoh, Y.; Souda, R. *Surf. Sci.* **2005**, *594*, 141.
- (10) Souda, R. *Phys. Rev. B* **2004**, *70*, 165412.
- (11) Cooks, R. G.; Ast, T.; Mabud, A. Md. *Int. J. Mass Spectrom. Ion Processes* **1990**, *100*, 209.
- (12) Pradeep, T.; Shen, J. W.; Evans, C.; Cooks, R. G. *Anal. Chem.* **1999**, *71*, 3311.
- (13) Cooks, R. G.; Ast, T.; Pradeep, T.; Wysocki, V. H. *Acc. Chem. Res.* **1994**, *27*, 316.
- (14) Pradeep, T.; Ast, T.; Cooks, R. G.; Feng, B. *J. Phys. Chem.* **1994**, *98*, 9301.
- (15) Pradeep, T.; Riederer, D. E.; Hoke, S. H., Jr; Ast, T.; Cooks, R. G.; Linford, M. R. *J. Am. Chem. Soc.* **1994**, *116*, 8658.
- (16) Pradeep, T.; Patrick, J. S.; Feng, B.; Miller, S. A.; Ast, T.; Cooks, R. G. *J. Phys. Chem.* **1995**, *99*, 2941.
- (17) Pradeep, T.; Evans, C.; Shen, J.; Cooks, R. G. *J. Phys. Chem. B* **1999**, *103*, 5304.
- (18) Kang, H. *Acc. Chem. Res.* **2005**, *38*, 893.

- (19) von Keudell, A.; Jacob, W. *Prog. Surf. Sci.* **2004**, *76*, 21.
- (20) Hopf, C.; von Keudell, A.; Jacob, W. *J. Appl. Phys.* **2003**, *94*, 2373.
- (21) Hopf, C.; von Keudell, A.; Jacob, W. *Nucl. Fusion* **2002**, *42*, L27.
- (22) Andersson, P. U.; Nagard, M. B.; Bolton, K.; Svanberg, M.; Pettersson, J. B. C. *J. Phys. Chem. A* **2000**, *104*, 2681.
- (23) Perry, C. C.; Faradzhev, N. S.; Fairbrother, D. H.; Madey, T. E. *Int. Rev. Phys. Chem* **2004**, *23*, 289.
- (24) Bianco, R.; Hynes, J. T. *Acc. Chem. Res.* **2006**, *39*, 159.
- (25) Buch, V.; Sadlej, J.; Aytemiz-Uras, N.; Devlin, J. P. *J. Phys. Chem. A* **2002**, *106*, 9374.
- (26) Petrenko, V. F.; Whitworth, R. W. *Physics of Ice*; Oxford University Press: New York, 1999.
- (27) Blanchard, J. L.; Roberts, J. T. *Langmuir* **1994**, *10*, 3303.
- (28) Grecea, M. L.; Backus, E. H. G.; Pradeep, T.; Kleyn, A. W.; Bonn, M. *Chem. Phys. Lett.* **2004**, *385*, 244.
- (29) Aoki, M.; Ohashi, Y.; Masuda, S. *Surf. Sci.* **2003**, *137*, 532–535.
- (30) Usharani, S.; Srividhya, J.; Gopinathan, M. S.; Pradeep, T. *Phys. Rev. Lett.* **2004**, *93*, 048304.
- (31) Cyriac, J.; Pradeep, T. *Chem. Phys. Lett.* **2005**, *402*, 116.
- (32) Stevenson, K. P.; Kimmel, G. A.; Dohnálek, Z.; Smith, R. S.; Kay, B. D. *Science* **1999**, *283*, 1505.
- (33) Zondlo, M. A.; Onasch, T. B.; Warshawsky, M. S.; Tolbert, M. A.; Mallick, G.; Arentz, P.; Robinson, M. S. *J. Phys. Chem. B* **1997**, *101*, 10887.
- (34) Trakhtenberg, S.; Naaman, R.; Cohen, S. R.; Benjamin, I. *J. Phys. Chem. B* **1997**, *101*, 5172.
- (35) Park, S. C.; Maeng, K. W.; Pradeep, T.; Kang, H. *Angew. Chem., Int. Ed.* **2001**, *40*, 1497.
- (36) Souda, R. *J. Phys. Chem. B* **2004**, *108*, 283.
- (37) Suter, M. T.; Bolton, K.; Andersson, P. U.; Pettersson, J. B. C. *Chem. Phys.* **2006**, *326*, 281.
- (38) Lee, C. W.; Lee, P. R.; Kang, H. *Angew. Chem., Int. Ed.* **2006**, *45*, 5529.
- (39) McClure, S. M.; Safarik, D. J.; Truskett, T. M.; Mullins, C. B. *J. Phys. Chem. B* **2006**, *110*, 11033.
- (40) Yue, Y. Z.; Angell, C. A. *Nature* **2004**, *427*, 717.
- (41) Torrie, B. H.; Weng, S. X.; Powell, B. *Mol. Phys.* **1989**, *67*, 575.
- (42) Brown, D. E.; George, S. M.; Huang, C.; Wong, E. K.; Rider, K. B.; Smith, R. S.; Kay, B. D. *J. Phys. Chem.* **1996**, *100*, 4988.
- (43) Holmes, N. S.; Sodeau, J. R. *J. Phys. Chem. A* **1999**, *103*, 4673.